TI Designs

1º Dial Using the LDC1314 Inductance-to-Digital Converter

1 Trademarks

All trademarks are the property of their respective owners.

TI Designs

TI Designs provide the foundation that you need including methodology, testing and design files to quickly evaluate and customize the system. TI Designs help *you* accelerate your time to market.

Design Resources

TIDA-00508	Tool Folder Containing Design Files
LDC1314	Product Folder
MSP430F5528	Product Folder
LP2985-N	Product Folder
TPD4E004	Product Folder

TI E2E™ Community

ASK Our E2E Experts
WEBENCH® Calculator Tools

Design Features

- Simple, Low-Cost Solution for Rotational or Lateral Position Sensing
- Robust Against Dirt, Dust, Moisture, and Oil
- Angular Position Sensing with 1º Absolute Accuracy and 0.1º Resolution
- Lateral Position Sensing With 0.3% Absolute Accuracy and 0.03% Resolution
- Differential Design Minimizes Z-Axis Sensitivity
- Algorithm Uses Minimal MCU Resources
- Features Three Calibration Methods
- Completely FR4 PCB-Based Design

Featured Applications

- Control Dials and Knobs
  - Home Appliances
  - Audio Equipment
  - Automotive Infotainment Systems
- Absolute and Incremental Encoders
- Industrial HMI

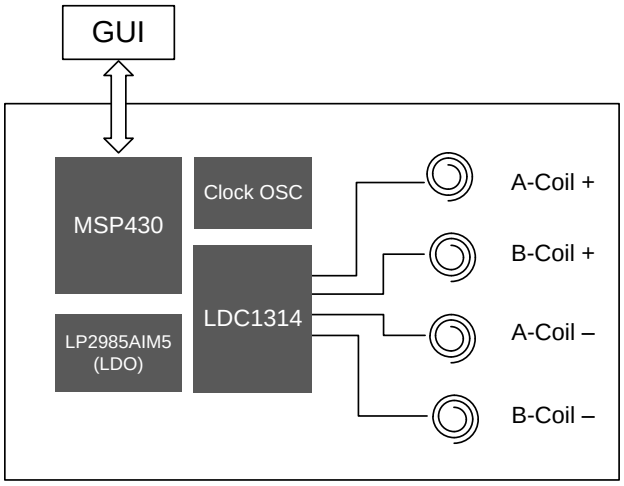

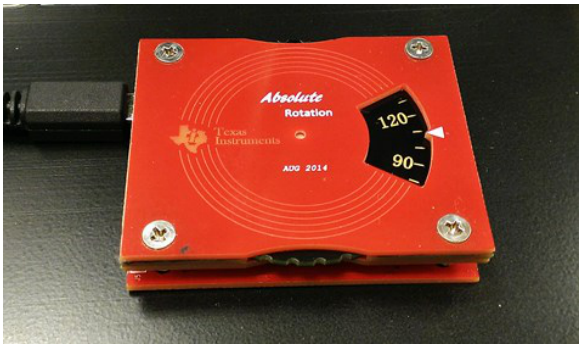

An IMPORTANT NOTICE at the end of this TI reference design addresses authorized use, intellectual property matters and other important disclaimers and information.

2 Overview

Historically, control dials have been implemented using predominantly mechanical contact-based systems. These systems are prone to break down and consequently expensive replacement over their lifetimes due to the moving parts. Alternate solutions using optical sensing are not immune to dirt and dust, which is a constraint for many industrial applications.

Inductive sensing is a contactless sensing technology that offers a more durable control dial implementation. Furthermore, this technology is extremely resistant to harsh environments along with being water and dirt proof as well. The TIDA-00508 offers a low cost, robust, absolute rotation, and lateral sensing solution targeted for implementing knobs, dials, and encoders in various industrial, consumer, and automotive applications.

To learn more about inductive sensing, go to www.ti.com/ldc.

3 Key System Specifications

This design consists of the dial assembly, the MCU board, and the GUI software. The key specifications include the following:

- Physical dimensions: 60.5 × 48.5 × 10 mm
- Dial disc diameter: 50 mm
- Diameter of the printed metal target: 26 mm
- Sensor coil diameter: 8 mm
- Sensor coil inductance: 3 μH
- Distance between sensors and target: 0.52 mm
- Angular position accuracy: See Table 1

Table 1. Dial Design Key Specifications

CALIBRATION METHOD	ACCURACY(1)	TEMPERATURE RANGE(2)
4-point	0.9°	0°C to 85°C
1-turn	1.8°	
Dynamic	10° initially 1.8° after one turn of use	
Off	3°	

(1) Based on alignment with naked eye
(2) Verified on 8-point naked-eye alignment

- Angular position resolution: < 0.1°
- Maximum rotation speed with 1° accuracy: 200 rpm
- Operating temperature: 0˚C to 85˚C
- Interface: USB on micro USB cable
- Power supply: 5 V (from USB)
- Total operating power consumption (including MCU): 30 mA

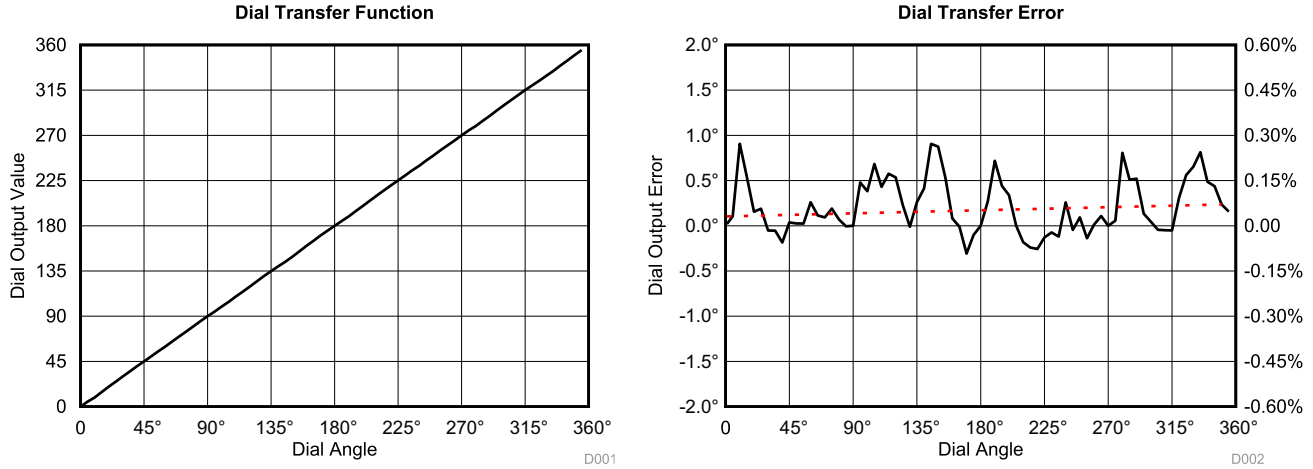

Figure 1. Typical Performance

4 System Description

The 1° Dial is an example of lateral proximity sensing using TI's LDC devices.

The basic principle of position sensing used in the dial is related to the phenomenon of eddy currents. When a metal is placed in close proximity to the coil of an oscillating LC tank, the induced current in the metal produces a counter field that reduces the effective inductance of the coil, thus changing the resonant frequency. The LDC1314 detects the inductance change by measuring the resonating frequency of the LC tank, thus measuring the proximity or overlap between the coil and the target metal. When the target metal is designed such that the amount of the coil-target overlap changes as the target rotates or shifts, rotational or linear movement of the target can then be measured, respectively. In the 1° dial, a rotating target is used for rotational position sensing.

The differential arrangement of the sensors helps minimize unwanted output change due to temperature, alignment, and z-axis tolerance and makes the board-to-board variation under three degrees without calibration.

The LDC passes the frequency data to an MSP430, which in turn communicates with a host platform, such as a PC, sending the frequency data to the host.

The dial in this design is constructed using a common FR4 PCB, screws, bolts, spacers, and washers. The GUI software reads the raw data from the dial hardware through USB, processes the data, and uses the result to animate the rotation angle graphically. It also displays the incremental position over multiple turns.

4.1 Block Diagram

The block diagram of the dial system is shown in Figure 2.

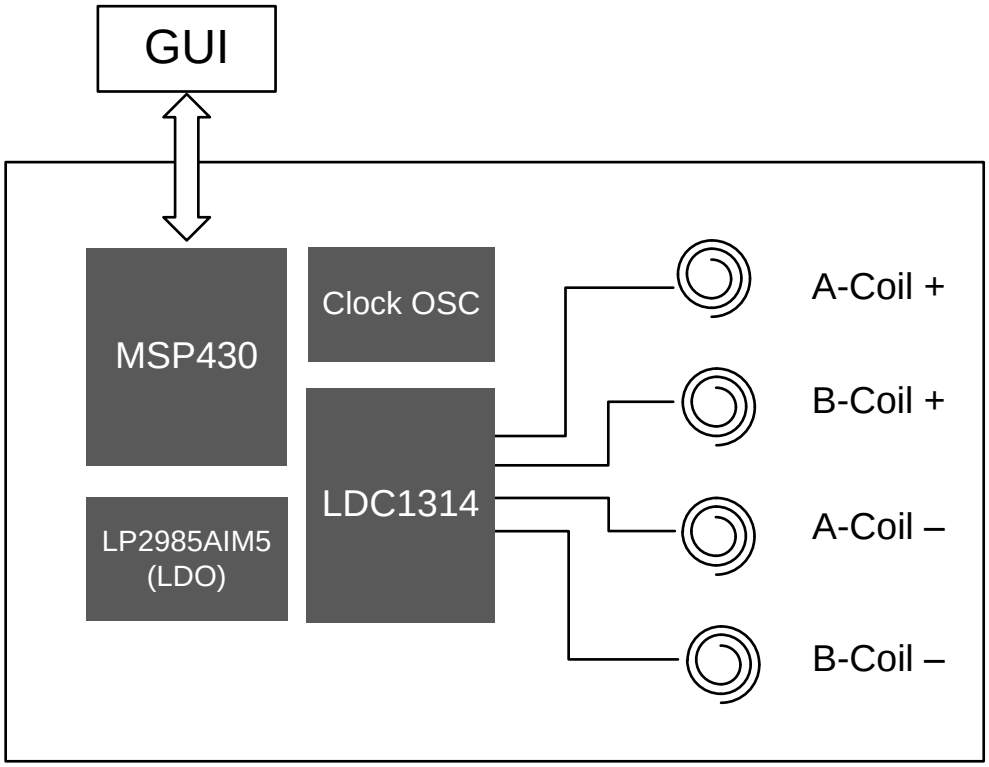

Figure 2. System Block Diagram

The system consists of the LDC1314 inductance-to-digital converter, the MSP430 microcontroller, and the supporting electronics. The microcontroller acts as a bridge between the I^2C interface of the LDC1314 and the GUI's USB COM port. It also provides nonvolatile storage for the initial register values of the LDC1314 as well as the calibration data.

The GUI software processes the data and displays the result graphically. It also handles the calibrations. These algorithms can be easily ported into a microcontroller for standalone applications.

The four sensor coils are grouped into two sets: Coil set A and coil set B, as shown in Figure 3. The two coils in each set form a differential sensor pair; the difference of their converted output is used by the system.

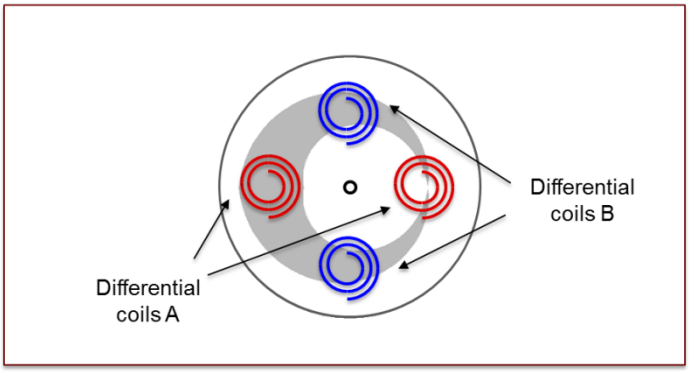

Figure 3. Differential Coil Sets

4.2 LDC1314

The LDC1314 is a four-channel inductance-to-digital converter. The four channels are connected to four sensor LC resonators, or LC tanks, each consisting of a PCB coil (L) and parallel capacitor (C). The output of each converter channel is a stream of 12-bit samples of the LC tank frequency on the selected channel. The I^2C serial interface provides access to the channel sample streams, usually from a microcontroller.

Figure 4 shows the LDC1314 functional block diagram. The sensors are attached to channels IN0A/IN0B through IN3A/IN3B. A high-frequency reference clock can be injected at the CLKIN pin, or the internal reference oscillator may be used. This reference clock (F_{REF}) is required to measure the sensor frequency (F_{SENSOR}). The LDC1314 is configured to measure F_{SENSOR} over a fixed number of F_{REF} periods, designated as REFCNT.

For more details, refer to the LDC1314 datasheet.

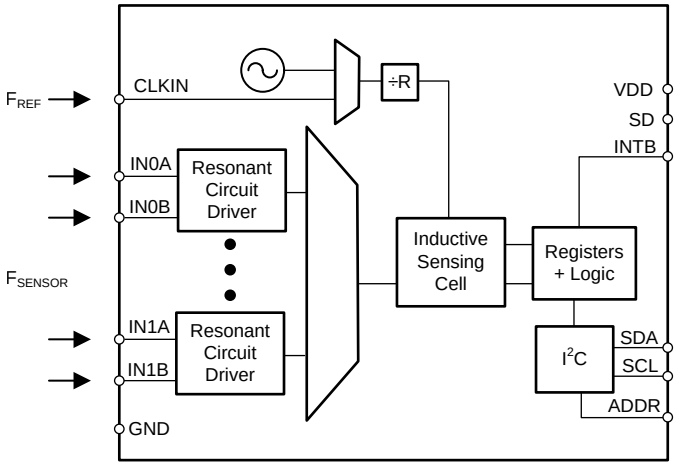

Figure 4. LDC1314 Functional Block Diagram

4.3 Other TI Parts

An MSP430 microcontroller is used as a bridge between the LDC1314 and the USB port. It also provides the non-volatile memory for the dial's calibration data.

An LP2985 low-dropout linear regulator is used to step down the 5-V USB power to the 3.3 V required by the LDC1314 and the MSP430.

To protect the demo board circuit from a possible ESD surge, the demo board uses a TPD4E004, the ESD protection circuit for high-speed data lines.

4.4 Mechanical Assembly

Figure 5 shows the mechanical construction of the dial.

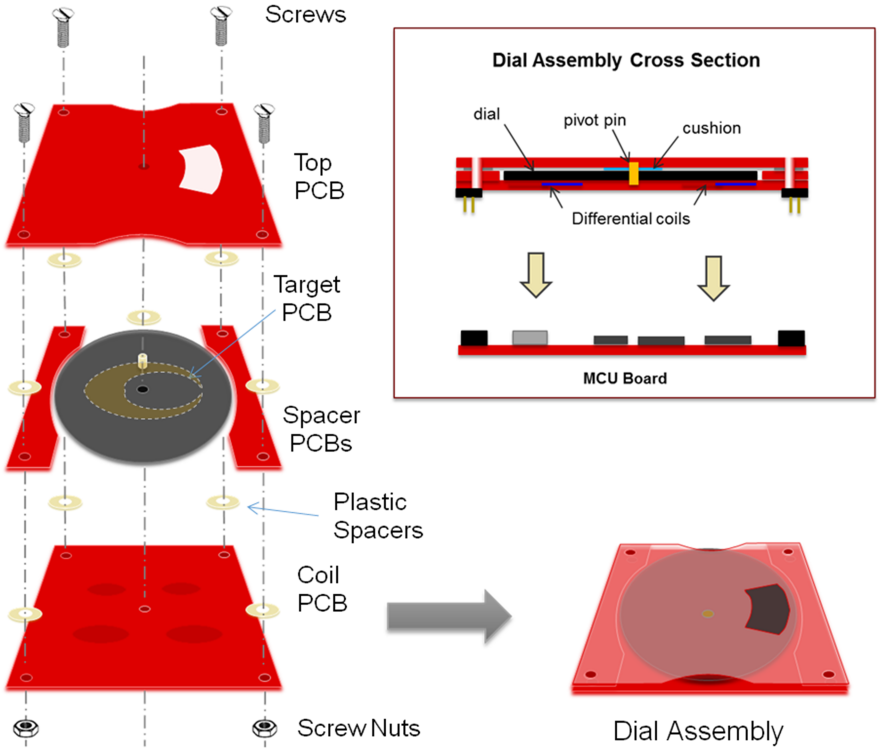

Figure 5. Mechanical Construction

5 System Design Theory: General Guide for Inductive Sensing Using LDC1314

The working principle of the LDC1314 is based on the phenomenon that the inductance of a coil reduces as it approaches a metal target. Various position sensing techniques have been developed based on this phenomenon.

5.1 Working Principles

The working principle of the LDC1314 is based on the phenomenon that occurs when a conductive material, such as a metal, is placed in a magnetic field. An AC current flowing through an inductor will generate an AC magnetic field. If a conductive material, such as a metal object, is brought into the vicinity of the inductor, the magnetic field will induce a circulating current (eddy current) on the surface of the conductor. The eddy current is a function of the distance, size, and composition of the conductor. The eddy current generates its own magnetic field, which opposes the original field generated by the sensor inductor. This effect is equivalent to a set of coupled inductors, where the sensor inductor is the primary winding and the eddy current in the target object represents the secondary winding. The coupling between the inductors is a function of the sensor inductor, and the resistivity, distance, size, and shape of the conductive target. The resistance and inductance of the secondary winding caused by the eddy current can be modeled as distance dependent resistive and inductive components.

Figure 6(a) shows an electrical model. The primary side represents the electrical model of a coil with series resistance (R_S), parasitic capacitance (C_{PAR}), and current I_1. The secondary side represents the target model, with eddy current I_2. The mutual inductance [M(d)] between the primary and secondary sides is a function of the distance between the two. Based on the dot convention, the voltage across the primary coil, V_P, is given by:

$$V_P(d) = L_S \frac{dI_1}{dt} - M(d) \frac{dI_2}{dt} \quad (1)$$

As the distance between the sensor coil and the target decreases, the mutual inductance M(d) increases, and the magnetic field strength at the surface of the target increases, increasing I_2. Because both M and I_2 increase, the total voltage across the primary side decreases. *Looking into the terminals of the primary side, this appears as a reduction in the effective inductance.*

An equivalent, parallel R-L-C model of the sensor and target can be constructed, as shown in Figure 6(b). Both the inductance and resistance vary with the distance between the target and sensor coil. The parallel equivalent circuit becomes a parallel resistor at parallel resonance, when the impedance of the parallel inductance is equal to that of the parallel capacitance in value at the parallel resonant frequency.

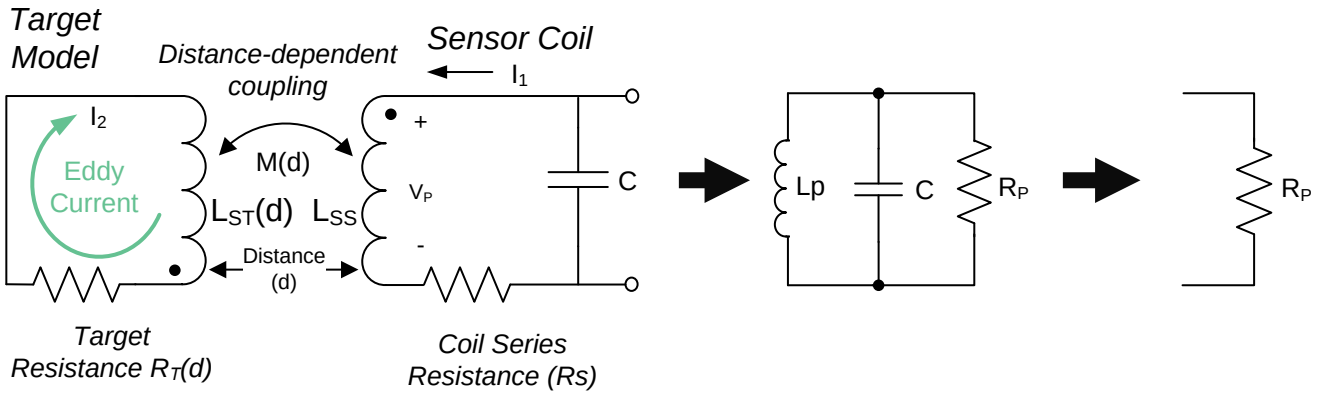

(a) Model for sensor and target (b) Parallel resonator model (c) Model at resonance

Figure 6. Electrical Model of the L-C Tank Sensor

The conversions from the series inductance and resistance into their parallel counterpart are listed in Table 2.

Table 2. Converting Series Resonator into Parallel Resonator

	SERIES RESONATOR → PARALLEL RESONATOR	
INDUCTANCE	L_S	$L_P = L_S (1 + Q_S^{-2})$
RESISTANCE	R_S	$R_P = R_S (1 + Q_S^{2})$
QUALITY FACTOR	$Q_S = \omega L_S / R_S$	$Q_P = R_P / \omega L_P$

An EM field can be generated using an L-C resonator, or L-C tank. One topology for an L-C tank is a parallel R-L-C construction, as shown in Figure 6(b). A parallel LC oscillator can be constructed by combining a frequency selective circuit with a gain block in a closed loop. The criteria for oscillation are: 1) loop gain greater than 1, and 2) closed loop phase shift of 2π radians. In the context of an oscillator, the R-L-C resonator provides the frequency selectivity and contributes to the phase shift. At resonance, the parallel impedance of the reactive components (L and C) cancels; leaving only RP, the lossy (resistive) element in the circuit. L and R are modeled as distance dependent components, and C includes both a parallel capacitance and the parasitic capacitance between the windings of the inductor.

The sensor oscillation frequency F_{SENSOR} is given by:

$$F_{SENSOR} = \frac{1}{2\pi\sqrt{LPC}} \tag{2}$$

Because the effective parallel inductance, L_P, decreases as the target moves closer to the sensor coil, Equation 2 tells us that the resonant frequency of the sensor increases.

Various position sensing techniques have been developed based on this phenomenon.

5.2 Sensor-Target Configuration

To design an inductive sensing application, the first step is to convert the desired measurement into the amount of exposed metal from a target in the electromagnetic field generated by the coils. Commonly used methods include axial proximity and lateral proximity, as depicted in Figure 7. As the metal target moves closer to the sensor coil, or the metal target shape covers more of the coil, a greater portion of the electromagnetic field is intercepted. The eddy current increases as more electromagnetic field flux are intercepted, decreasing the effective inductance of the coil generating the field and increasing the LC tank oscillation frequency. This result leads to a greater digital output value from the LDC131x and LDC161x.

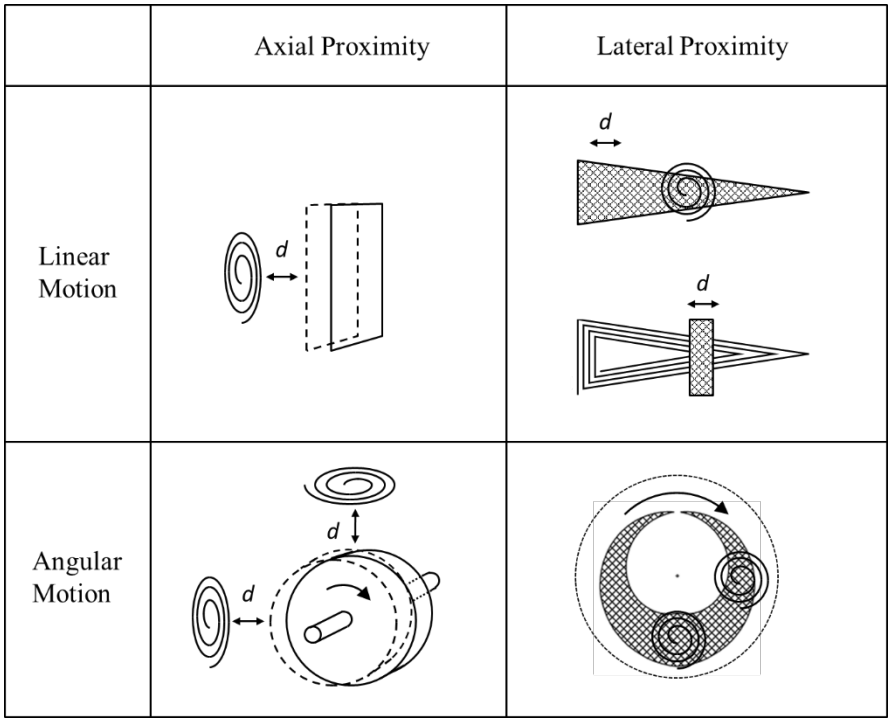

Figure 7. Commonly Used Sensor-Target Configurations

In some position sensing cases, a single coil is sufficient. Multiple coils can obtain differential data to cancel certain unwanted variances due to temperature or mechanical tolerances. In rotational sensing, the use of multiple coils enables continuous 360-degree angular position sensing, and can also increase the sensing accuracy.

5.3 Target Metal: Composition and Thickness

Certain metal types perform better than other types in terms of creating greater sensor output change. These metals have a high electrical conductivity and a low magnetic permeability, for example, common aluminum (alloys) and copper (alloys). The 300 series of non-ferrite stainless steel materials (that is, it cannot be picked up by a magnet) also works well.

Because alternating currents (such as eddy currents) tend to concentrate on the metal surface facing the sensor coil (known as the "skin effect"), a thin layer of metal usually works well enough. Table 3 shows the recommended minimum thickness for several commonly used metals.

Table 3. Recommended Minimum Target Metal Thickness (µm)

TARGET METAL	SENSOR FREQUENCY		
	1 MHz	3 MHz	10 MHz
Copper	63	37	20
Silver	64	37	20
Gold	77	45	24
Aluminum	82	47	26
Aluminum alloy	99	57	31
Brass (yellow)	127	73	40
Solder	214	123	68
Non-ferritic stainless steel (3xx series)	421	243	133

5.4 Coil Design Information

The wide range of oscillation frequency and the driving current of the LDC131x and LDC161x gives the user great flexibility in selecting the dimensions of the coil that best suits their mechanical system configuration. However, certain rules must be followed to ensure the proper operation of the IC.

- *LC tank resonant frequency* — The recommended sensor frequency range for LDC131x and LDC161x devices is 1 kHz to 10 MHz.
- *Inductance of the sensor coil* — There is no absolute requirement on the value of the inductance as long as the range of the resonant frequency and R_P (the parallel loss resistance) are not violated.
- *Sensor oscillation amplitude* — The maximum allowable sensor oscillation amplitude must not exceed 1.8 V. The maximum operating amplitude occurs when the target is either at its maximum distance from the sensor coil (axial sensing) or the least amount of target area overlaps the coil (lateral sensing). The minimum amplitude occurs when the target is at its closest point to the sensor (axial), or when is achieves maximum overlap with the coil (lateral). The datasheet recommends that the minimum operating amplitude be maintained above 500 mV. As already explained, the sensor voltage is proportional to $R_P(d)$, which will vary as the target moves. Therefore, the coil must be carefully designed to maintain a sufficient range of R_P over the operating range to ensure that the sensor oscillation does not collapse.
- *R_P (Parallel Loss Resistance) of the LC tank* — As described in Section 5.1, the LC tank is "lossy" due to the inductor's loss and the energy dissipated by the target metal. This loss can be modeled by a parallel equivalent resistance R_P. The more the energy loss in the LC tank, the smaller the value of R_P. The range of R_P values that the LDC131x and LDC161x devices can handle is from 150 Ω to 100 kΩ, with gradually degrading S/N as it decreases below 1 kΩ. Although it is possible for R_P to exceed 100 kΩ, the minimum R_P value is more important in a majority of applications. Higher "open-air" R_P (that is, R_P value measured with no target metal) helps increase the S/N of the output. To increase the open-air R_P, use thick trace size for the printed sensor coil. Appendix A described three methods for measuring R_P value of an inductor.

5.5 Interpreting and Using the Output Data

The digital output of the LDC131x and LDC161x is a number proportional to the LC tank's oscillating frequency:

$$D = \frac{F_{TANK}}{F_{REF}} \times 2^{N} \quad (3)$$

where

- N is 12 for LDC131x and 28 for LDC161x

Note that $F_{TANK} = F_{SENSOR}$. The tank frequency is monotonically related to the proximity between the sensor coil and the target metal. Because F_{REF} and N are constant, D can be directly used to indicate the target position.

D is a monotonic function of the proximity. In axial sensing, D increases as the distance decreases. In lateral sensing, D increases as the target moves such that more metal overlaps the coil. In almost all cases, D is not a linear function of the proximity distance. To derive the position from D, two methods can be used, Table Look-up and Template Fitting, as explained below.

- Table look-up method — The look-up table is a table of D values at discrete position values X, and is obtained experimentally from a real system. The table is then used to find the target position X from any D value. For any D value that is not in the table (a most likely situation), either the most adjacent D value can be used, or the actual distance value can be calculated by interpolating the two adjacent X values.
- Template fitting method — In this method, sensors and target are designed such that the output function D = f(X) closely approximates some known mathematical function. The X can then be calculated using the inverse function X = f(D). One example of the template fitting method is described in Section 5.

5.6 Resolution of the Position Measurement

The resolution of a position sensing system is defined as the number of discrete position values that the sensor can resolve within the measurement range. In the LDC131x and LDC161x, the resolution is directly related to how finely the LC tank frequency can be resolved. Suppose the LC tank frequency increases from F_1 to F_2 as a result of moving the target from position P_1 to P_2. The position resolution is then:

$$\text{Steps between } P_1 \text{ and } P_2 = 32 \times \text{REFCNT} \times \frac{\Delta F_{TANK}}{\text{mean}\left(F_{TANK}\right)} = 64 \times \text{REFCNT} \times \frac{\left|F_1 - F_2\right|}{F_1 + F_2} \quad (4)$$

where

- REFCNT = reference clock count used to measure F_{TANK}. (See the LDC1314 datasheet)

Do not confuse this resolution with the number of bits in the output samples. In the case of the LDC161x, the output sample usually has enough bits to represent the effective resolution shown above. In the case of the LDC131x, because the output samples have only 12 bits, the internally available resolution is sometimes under-represented by the output sample, and the effective resolution can decrease. If this is the case, use the GAIN and OFFSET registers offered in the LDC131x to restore the resolution. Altering the reference frequency (including setting the REFDIV register) can also help recover the resolution. Also note that the ratio of the effective reference frequency to tank frequency must be greater than 4 for both the LDC131x and the LDC161x.

5.7 System-to-System Variation and System Calibration

System-to-system variations in practical applications do exist. This is mainly due to the component tolerances. The capacitors and the inductance of the coils are the main contributor to the system-to-system variation. Good quality capacitors, such as the NP0/C0G ceramic capacitors or film capacitors with tolerance of 1% to 5% are recommended. Non-printed sensor coils (inductors) should also have a tolerance of 5% or less.

For sensing systems that require a high accuracy, a system calibration will be necessary. One of the most common calibrations involves offset and gain calibration. In many systems, an on-the-fly calibration may be a good choice as it does not require permanent calibration data storage.

6 Quadrature Rotational Position Sensing

Rotational encoding in this system is implemented using a quadrature approach. Sensor coil sets A and B are placed 90 degrees from each other underneath the rotating target. This arrangement enables the detection of angle and rotation direction of the target. Set A is referred to as the "in-phase" (I) sensor set, and set B is referred to as the "quadrature" (Q) sensors set. The I-Q sensor arrangement is illustrated in Figure 8. The Data A and Data B traces represent the output waveforms that are derived from the sample streams.

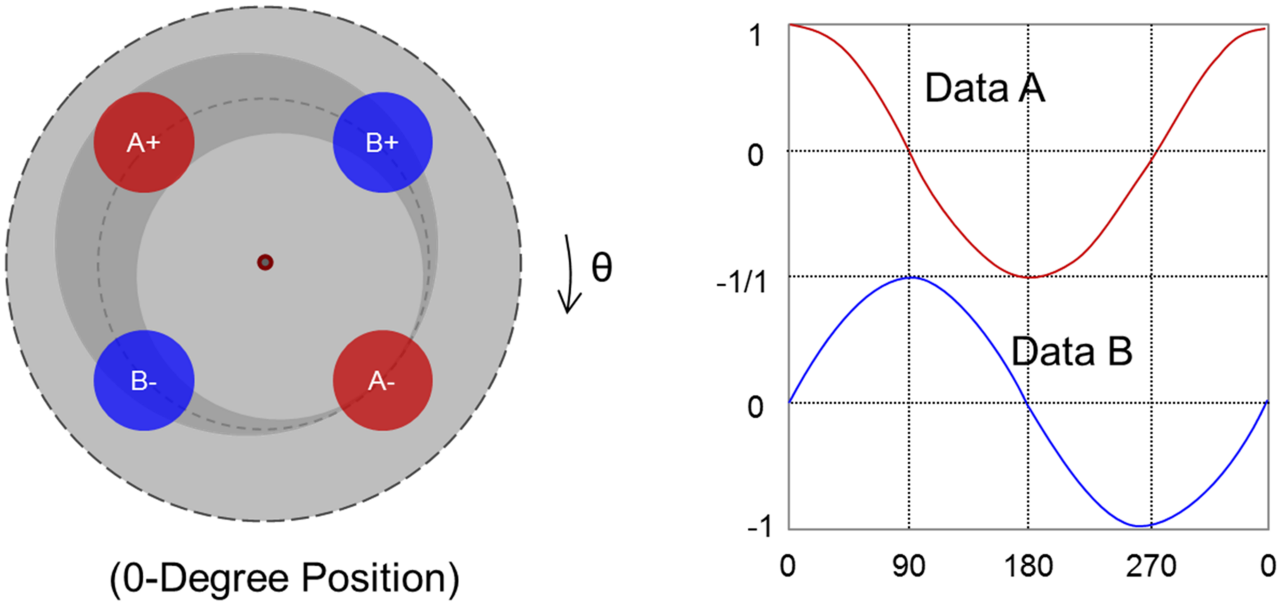

Figure 8. In-Phase and Quadrature Sensors

Data A is obtain by A = (Data A+) – (Data A–). Refer to the coil arrangement picture in Figure 8. At position $\theta = 0°$, coil A+ overlaps with the maximum amount of target area. This produces the maximum value in the output of the LDC1314. Coil A– overlaps with minimum amount of target area, giving the minimum output values. Therefore, the differential output A is at maximum. The output B is obtained in a similar manner. The differential data A and B are plotted against the target rotational angle in Figure 8. For each pair of data (A, B), there is a unique θ. Therefore, the I-Q sensor arrangement can measure the absolute rotation angle around 360˚.

As can be seen from the plot in Figure 8, the output data A and data B waveforms resemble cosine and sine functions. This enables the algorithm to use the trigonometric functions to process the data and find the rotation angle θ from data (A, B).

6.1 Data Processing

In the dial demo system, the data processing is done in the GUI software. The firmware in the MCU board reads the data from the LDC1314 and sends it to the GUI upon request. However, the algorithm in the GUI software can be ported to a microcontroller for stand-alone applications.

The data processing consists of the following stages:

- Linear corrections
  - Offset correction
  - Magnitude correction
- Shape correction (non-linear correction)
  - Exponential pre-distortion
- Rotation angle calculation
  - Inverse-trigonometric function (arctangent function)
- Phase skew correction
  - Weighted phase skew correction

The corrections are performed using calibration data collected during the calibration processes (described in Section 7). The data processing flow is illustrated in Figure 9.

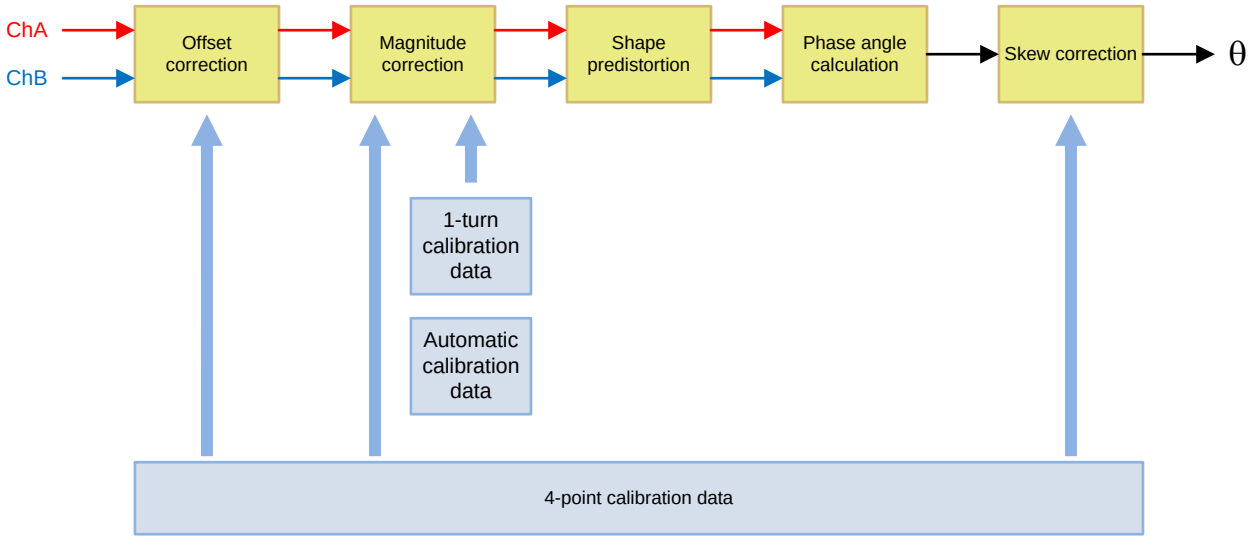

Figure 9. Data Processing Flow

6.1.1 Linear Correction

In the linear correction, both data A and B are first centered so that the positive and negative magnitudes are equalized. Then, the magnitudes are normalized to 1. Figure 10 illustrates the linear correction.

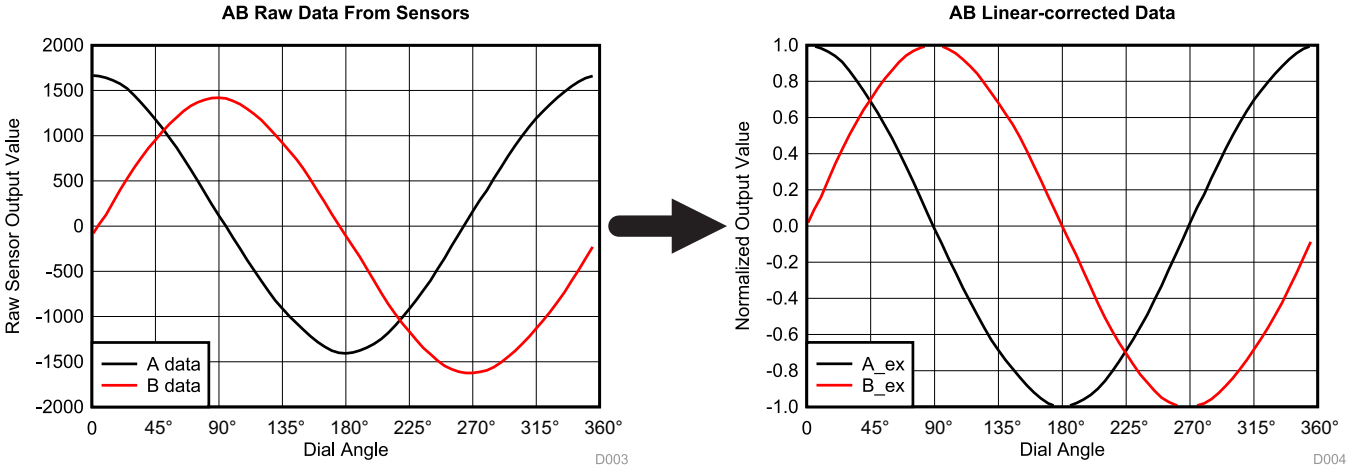

Figure 10. Linear Correction

6.1.2 Shape Pre-Distortion

After the linear correction, data A and B look much like the cos(θ) and sin(θ) functions, respectively. Data A and B can be further processed, or "pre-distorted", to improve their approximations to the cos(θ) and sin(θ) functions. In the dial algorithm, this is done by the nonlinear operation:

$$A = \text{sign}(A) \times \text{abs}(A)^{EXP}, \text{ and}$$

$$B = \text{sign}(B) \times \text{abs}(B)^{EXP} \quad (5)$$

where

- sign(x) and abs(x) are the standard sign and absolute value functions in any computer language

EXP is a number that affects the shape of the resulting waveform, as explained in Figure 11:

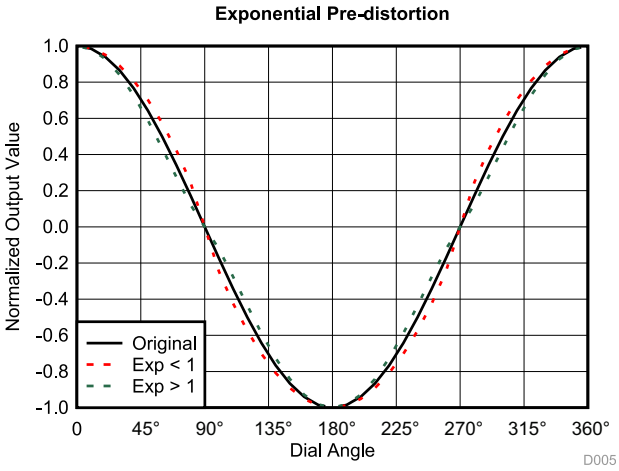

Figure 11. Waveform Shape Pre-Distortion

6.1.3 Phase Angle Calculation

In the phase angle calculation, the phase angle of data A and B are used to find the "electric phase angle" of the signal. In the dial implementation, there is only one I-Q sensor pair so one cycle of physical rotation corresponds to one cycle of the electric waveform. As mentioned in Section 6.1.2, the dial algorithm uses trigonometric functions as the template for decoding the position. After linear and nonlinear corrections, the A and B data are ready to be decoded for phase angle:

$$\theta = \begin{cases} \arctan\left(\frac{B}{A}\right) & \text{if } A \geq 0 \text{ and } B \geq 0 \\ \arctan\left(\frac{B}{A}\right) + 180^\circ & \text{if } A < 0 \\ \arctan\left(\frac{B}{A}\right) + 360^\circ & \text{if } A \geq 0 \text{ and } B < 0 \end{cases} \quad (6)$$

6.1.4 Phase Skew Correction

Due to the mechanical tolerances, and asymmetry in parasitic metal distribution around or near the sensors and so on, there are phase skew errors around the cycle. These skew errors can be corrected as the last step in the error correction. In the dial algorithm, the skew correction is done round the 360˚ circle by interpolating the four known skew correction points collected in the calibration, as explained by Figure 12:

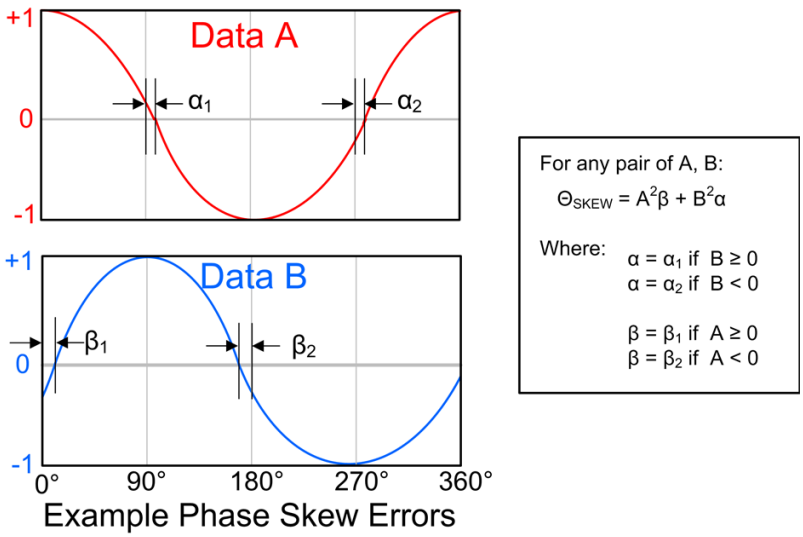

Figure 12. Skew Correction

The electric phase angle θ is then modified by:

$$\theta = \theta - A^2\beta - B^2\alpha \quad (7)$$

6.1.5 Final Result

There are 45 degrees of difference between the electric phase angle and the physical rotational angle because of the way the target and sensors are aligned physically. Counting this 45-degree offset between the electric phase angle and the physical rotational angle of the target results in:

$$\text{Rotation angle} = \theta + 45^\circ \quad (8)$$

7 Calibration Methods

The initial errors in the dial sensing systems come from the mechanical tolerance, coil inductance tolerance, capacitor tolerance, surrounding metals, and so on. Calibration can greatly reduce the sensing errors caused by these initial tolerance errors.

Generally, the calibration is carried out prior to the usage of the system. The data generated by the calibration process is then stored permanently in the system. During use, the data-processing algorithm uses the calibration data to eliminate the sensing error.

Certain applications allow for the calibration to be done "on-the-fly".

In the dial algorithm, three different options for calibration are included: the four-point calibration, the one-turn calibration, and the automatic calibration (or on-the-fly calibration). These calibration methods are described in the following sections.

7.1 4-Point Calibration

In four-point calibration, the sensor output data are collected at four special target positions: 45˚, 135˚, 225˚, and 315˚, corresponding to electric phase angles of 0˚, 90˚, 180˚, and 270˚. The peak and offset values are recorded as the calibration data. The four-point calibration is depicted in Figure 13.

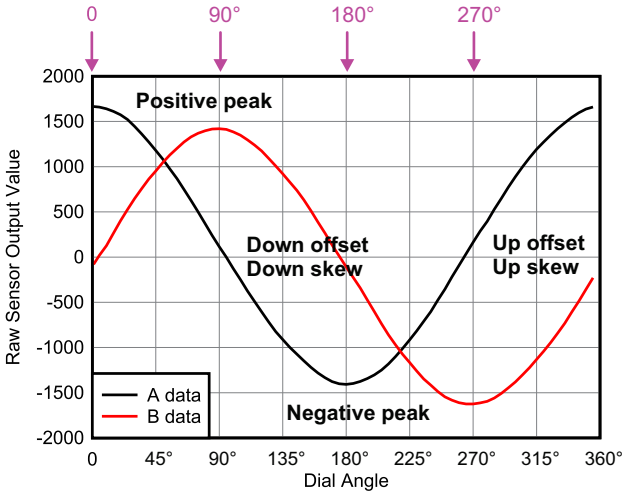

Figure 13. 4-Point Calibration

The peak and offset values are used in the linear correction stages in the data processing algorithm (refer to Section 6.1.1) to center and normalize the A, B waveforms.

In addition to the peaks and offsets, skew errors can also be derived from the four-point calibration. This is done by using the A and B data at the four calibration positions to find the angles using the formulas in Section 6.1.3. These four angles are the skews β_2, α_1, β_1, and α_2 in Figure 12. These skews are used by the algorithm to correct the phase angle skew.

7.2 1-Turn Calibration

In the one-turn calibration process, the target is rotated by a full turn, and the calibration data is automatically extracted by the GUI. No mechanical alignment is required, reducing the production cost.

As illustrated by Figure 14, the positive and negative peaks are recorded. These peaks are used by the data processing algorithm to do the linear correction. The skew correction will be skipped when the one-turn calibration is in effect. Because of this, the accuracy of the one-turn calibration is less than that of the four-point calibration.

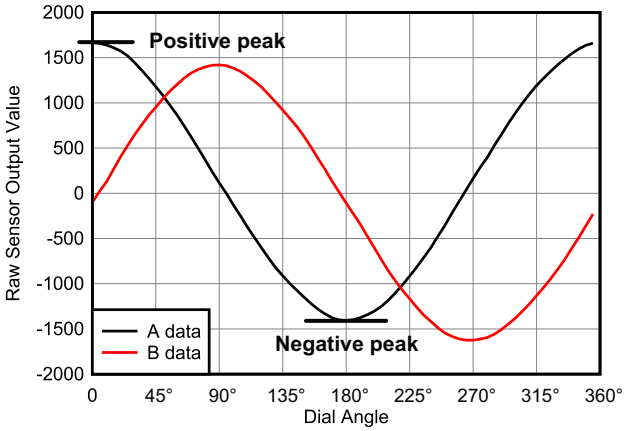

Figure 14. 1-Turn Calibration

7.3 Automatic Calibration

The Automatic Calibration mode is also referred to as Dynamic Calibration or On-the-Fly Calibration. In this mode, no calibration data is stored; the positive and negative peaks are updated at the time of operation, as illustrated in Figure 15. The advantage of the automatic calibration is that it requires neither production-time alignment nor system storage for the calibration data, minimizing the overall system cost. The same accuracy of the one-turn calibration is reached after one net turn of use.

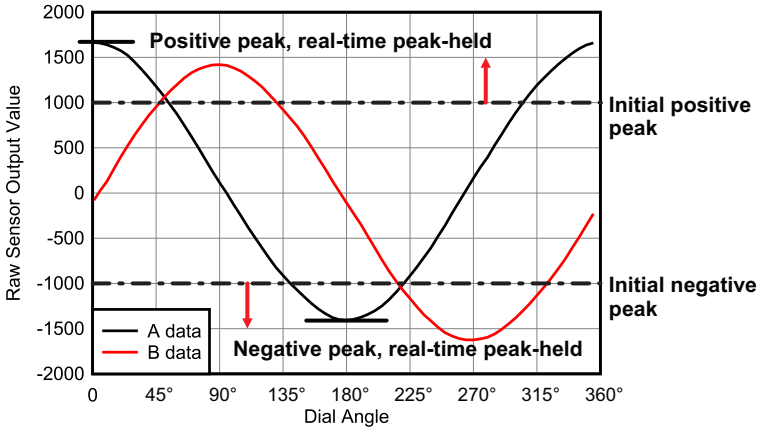

Figure 15. Automatic Calibration

7.4 Summary of Calibration Modes

Table 4 summarizes the calibration modes implemented in the dial algorithm. Different applications can choose the calibration that best meets the requirements of use case, accuracy, and cost.

Table 4. Comparison of Calibration Modes

CALIBRATION METHOD	CALIBRATION ITEMS	ACCURACY AND STABILITY	RESOURCE REQUIREMENT	
			NV STORAGE	ALIGNMENT
4-point	Magnitude and skew	Best	Required	Required
1-turn	Magnitude	Good	Required	Not required
Dynamic	Magnitude	Good after one turn of use	Not required	Not required
Off	None	Less than good	Not required	Not required

8 Sensor and Target Design

The LDC1314 measures the sensor oscillation frequency to determine the position of the target. The sensor design, therefore, plays the most important role in the success of the sensing system. The basic sensor design approaches are discussed in the following sections.

8.1 Sensor-Target Physical Arrangement

The essence of a good inductive sensor is to create a high degree of controlled electromagnetic induction between the sensor and the target. The dial implementation uses the "lateral sensing" technique, where the sensors (coils) and the target are placed parallel to each other. The distance between the sensor and target is fixed, but lateral position changes. The overlapped area between the coil and the target determines the amount of field interception, which in turn changes the eddy current strength, altering the mutual inductance between the sensor and target, causing a frequency shift in the sensor, as described in Section 5.1. The frequency shift, therefore, can be used to indicate the lateral movement between the coil and the target. Because the distance between the coil and the target also changes the field interception, it is very important to keep this distance constant at all times in order to produce reliable lateral position sensing.

The design of the dial assembly guarantees a constant distance between the sensor coil and target by placing the target disc in contact with the coil board, as illustrated in Figure 16.

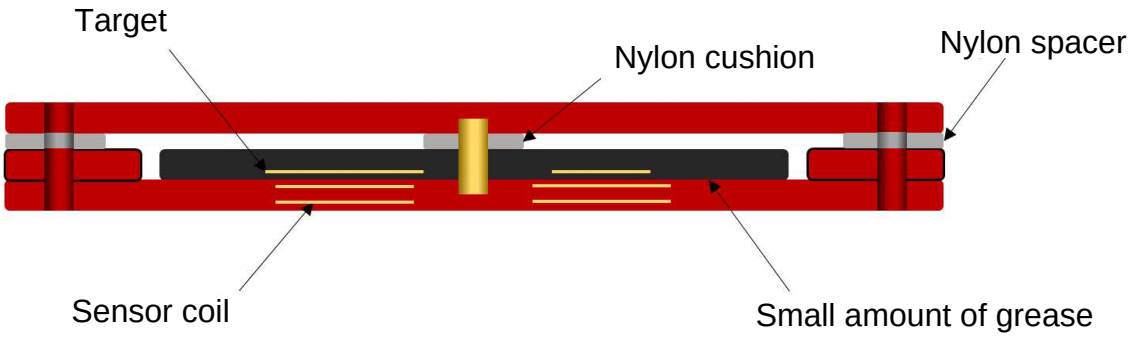

Figure 16. Sensor-Target Spacing

8.2 Sensor Coil Design

The four sensor coils are printed on the inner layers, layer 2 and layer 3, of the coil board. Each coil contains two layers of printed spiral coils, connected in series to maximize the inductance. Each coil is 8 mm in diameter and contains 14 turns per layer. The nominal inductance is 3 μH. This inductance is chosen because it is larger than the smallest recommended inductance for the LDC1314 so that the operation is small enough to fit the target size well. The coil diameter is similar to the widest width of the target to ensure full overlap. Refer to the PCB design file for copper and layer stacking details.

The tank capacitor is a 180-pF, 1% ceramic SMD part. These values make the tank oscillate at around 8.5 MHz nominally, below the 10-MHz operation limit. It is advantageous to have the sensor working at the highest possible frequency in precision applications such as the dial, because a fewer number of turns are required (frequency $\propto 1/N^2$). Also, fewer turns help to reduce the temperature drift of the frequency due to the target's resistance change.

Place the capacitors as close to the sensor coil as possible to reduce the parasitic inductance of the PCB traces. The trace length from the LC tank to the IC is less critical because they do not affect the resonance frequency.

To minimize the difference in inductance between the four coils, equalize the PCB trace lengths from the coil to the LDC1314.

The dial coil board is shown in Figure 17.

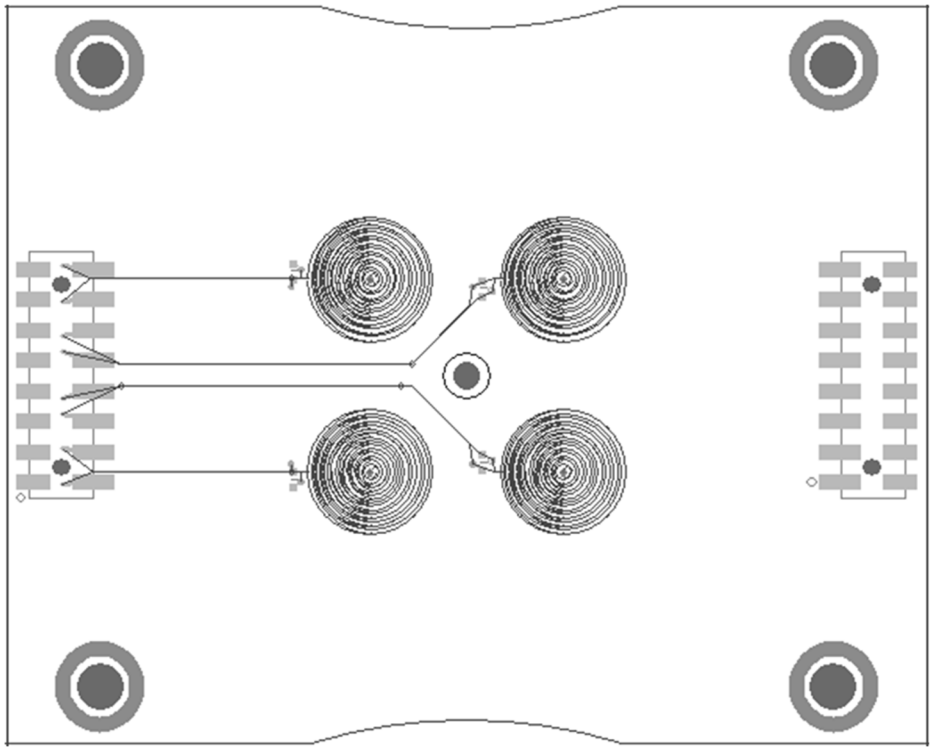

Figure 17. Coil Board

NOTE: Coils are printed in Layer 2 and Layer 3 of the four-layer PCB.

8.3 Target Design

The target metal is printed in the third layer of the dial's disc. The thickness of the copper pattern must be twice the skin depth of the signal. At a 9-MHz oscillating frequency, the skin depth on copper is about 20 μm. The target copper thickness should be greater than 40 μm. The 1-ounce copper has a thickness of 50 μm, satisfying the skin depth requirement.

The target pattern is a "Phase-Linear Width" pattern, because the radial width of the metal pattern is proportional to the phase angle, as explained in Figure 18.

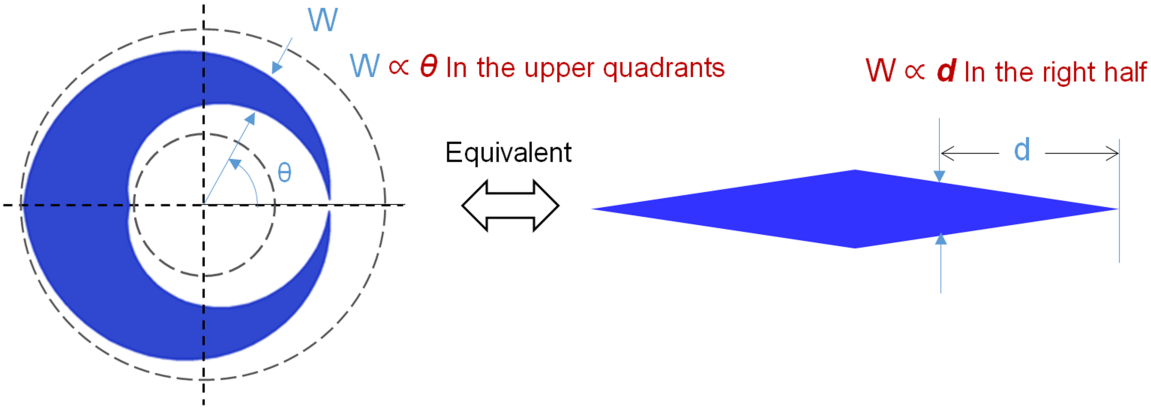

Figure 18. Target Shape

Place the coils around the circle centered at the rotation axis. The target should also be located concentric to this circle with the circle dividing the radial width of the target equally. The dimension of the target should be such that the coil diameter is 10% greater than the maximum width (at 180˚), and the radius of the common circle is 20% greater than the maximum width. Refer to Figure 19 for details.

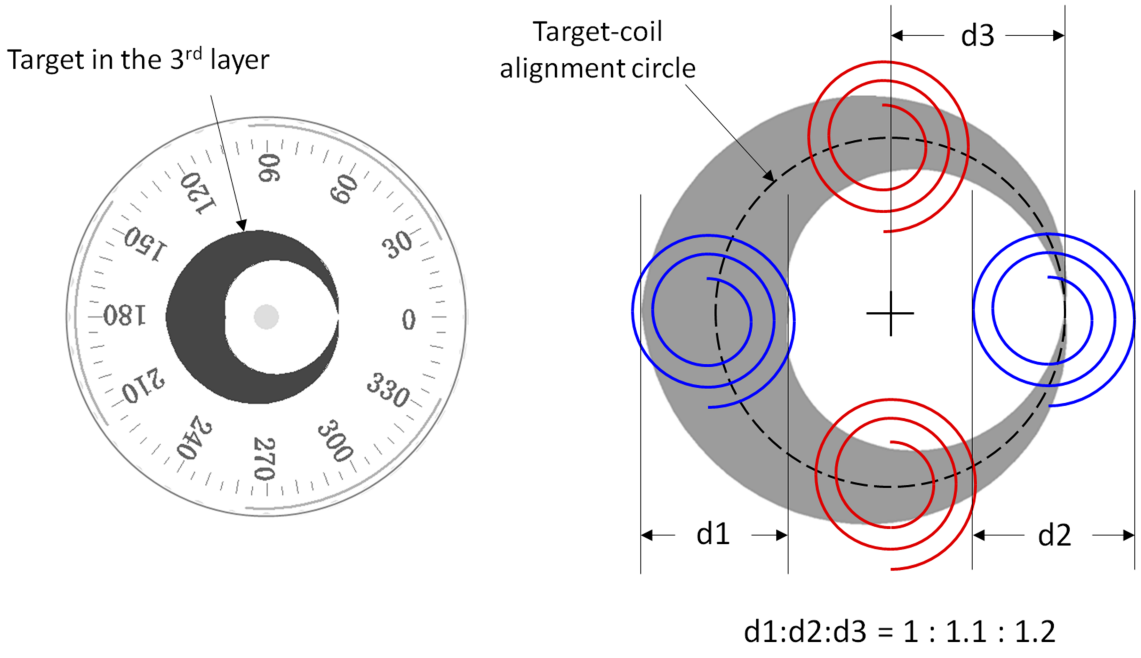

Figure 19. Target Disc and Target-Coil Alignment

A spreadsheet calculator is available to aid the target design using a PCB layout tool. The calculator determines the x-y coordinates of a piecewise linear target shape that can be used when drawing the target object. This calculator, Target Shape Calculator.xlsx, is included in the design guide package.

9 Firmware

9.1 Port Commands

The MSP430 firmware of the dial is a bridge between the LDC1314's I^2C interface and the virtual COM port of the GUI. The baud rate is 912.6k. There are six commands:

- *: This command requests the firmware to send the sensor output data, each 16-bit long, in the following sequence: Ch0, Ch1, Ch2, Ch3
- BW w w: Block-writes the 16-bit values that follow to the flash storage of the microcontroller, starting from address 0
- BR n: Requests the firmware to send n 16-bit values in the flash storage from address 0
- IW addr reg wwww: Writes the 16-bit value w into the reg register of the I^2C device having address addr
- IR addr reg: Requests the firmware to send the 16-bit content of register reg of the I^2C device having address addr
- LR: Loads the default register values into the LDC1314 registers (with I^2C address of 2 A)

The encoding of the mnemonics and parameters uses ASCII characters. The parameters are separated by a space character. Each command is terminated by a CR character. The returned values are also encoded in ASCII characters, with one exception: the "*" command. The returned value of the * command is not encoded.

9.2 Flash Storage Data Format

The flash memory dedicated to the dial firmware has the following assignment:

```
.equ    Flash_1614_R08,     0     ; Register 08
.equ    Flash_1614_R09,     2     ; Register 09
.equ    Flash_1614_R0A,     4     ; Register 0A
.equ    Flash_1614_R0B,     6     ; Register 0B
.equ    Flash_1614_R0C,     8     ; Register 0C
.equ    Flash_1614_R0D,     10    ; Register 0D
.equ    Flash_1614_R0E,     12    ; Register 0E
.equ    Flash_1614_R0F,     14    ; Register 0F
.equ    Flash_1614_R10,     16    ; Register 10h
.equ    Flash_1614_R11,     18    ; Register 11h
.equ    Flash_1614_R12,     20    ; Register 12h
.equ    Flash_1614_R13,     22    ; Register 13h
.equ    Flash_1614_R14,     24    ; Register 14h
.equ    Flash_1614_R15,     26    ; Register 15h
.equ    Flash_1614_R16,     28    ; Register 16h
.equ    Flash_1614_R17,     30    ; Register 17h
.equ    Flash_1614_R19,     32    ; Register 19h
.equ    Flash_1614_R1A,     34    ; Register 1Ah
.equ    Flash_1614_R1B,     36    ; Register 1Bh
.equ    Flash_1614_R1C,     38    ; Register 1Ch
.equ    Flash_1614_R1D,     40    ; Register 1Dh
.equ    Flash_1614_R1E,     42    ; Register 1Eh
.equ    Flash_1614_R1F,     44    ; Register 1Fh
.equ    Flash_1614_R20,     46    ; Register 20h
.equ    Flash_1614_R21,     48    ; Register 21h
```

Upon power up, these values are written into the intended LDC1314 registers. The LDC1314 registers can also be re-loaded by the LR command. Table 5 contains the register contents used for this application.

Table 5. LDC1314 Register Values

REGISTER ADDRESS	REGISTER NAME	REGISTER VALUE
0x08	RCOUNT_CH0	03AA
0x09	RCOUNT_CH1	03AA
0x0A	RCOUNT_CH2	03AA
0x0B	RCOUNT_CH3	03AA
0x0C	OFFSET_CH0	247B
0x0D	OFFSET_CH1	247B
0x0E	OFFSET_CH2	247B
0x0F	OFFSET_CH3	247B
0x10	SETTLECOUNT_CH0	4
0x11	SETTLECOUNT_CH1	4
0x12	SETTLECOUNT_CH2	4
0x13	SETTLECOUNT_CH3	4
0x14	CLOCK_DIVIDERS_CH0	0
0x15	CLOCK_DIVIDERS_CH1	0
0x16	CLOCK_DIVIDERS_CH2	0
0x17	CLOCK_DIVIDERS_CH3	0
0x19	ERROR_CONFIG	0
0x1A	CONFIG	1.00E+01
0x1B	MUX_CONFIG	C23F
0x1C	RESET_DEV	400
0x1E	DRIVE_CURRENT_CH0	D000
0x1F	DRIVE_CURRENT_CH1	D000
0x20	DRIVE_CURRENT_CH2	D000
0x21	DRIVE_CURRENT_CH3	D000

10 GUI Software

The GUI software is written in Visual Basic® 2012. The main screen is the graphic animation of the dial. In addition, there is one subscreen, USB.

10.1 Main Screen

The main screen is shown in Figure 20. Clicking the button on the lower right toggles through the four calibration modes of the dial data processing, which are described in Section 7.

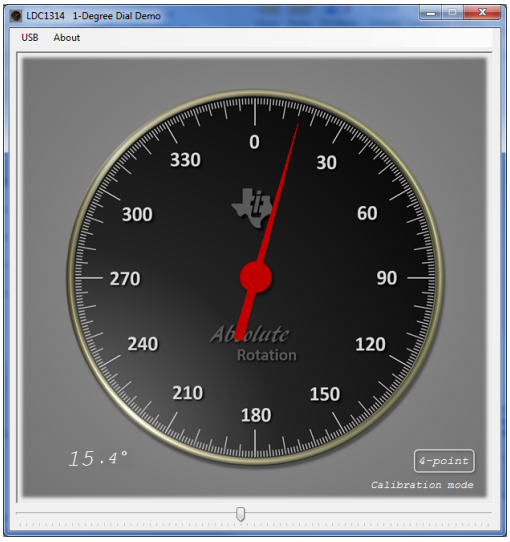

Figure 20. GUI Main Screen

10.2 USB Screen

The COM port is selected in the USB screen. The COM port must be selected first for the proper operation of the dial. The USB screen is shown in Figure 21.

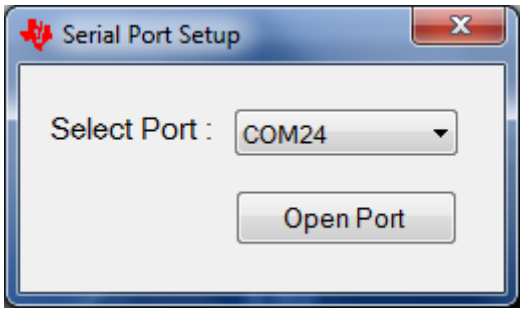

Figure 21. USB Screen

11 Test Data

The dial has been tested between 0°C and 85°C and demonstrated good stability. The test results match what is shown in Table 1 and Figure 1.

12 Design Files

12.1 Schematics — MCU Board

To download the schematics, see the design files at TIDA-00508.

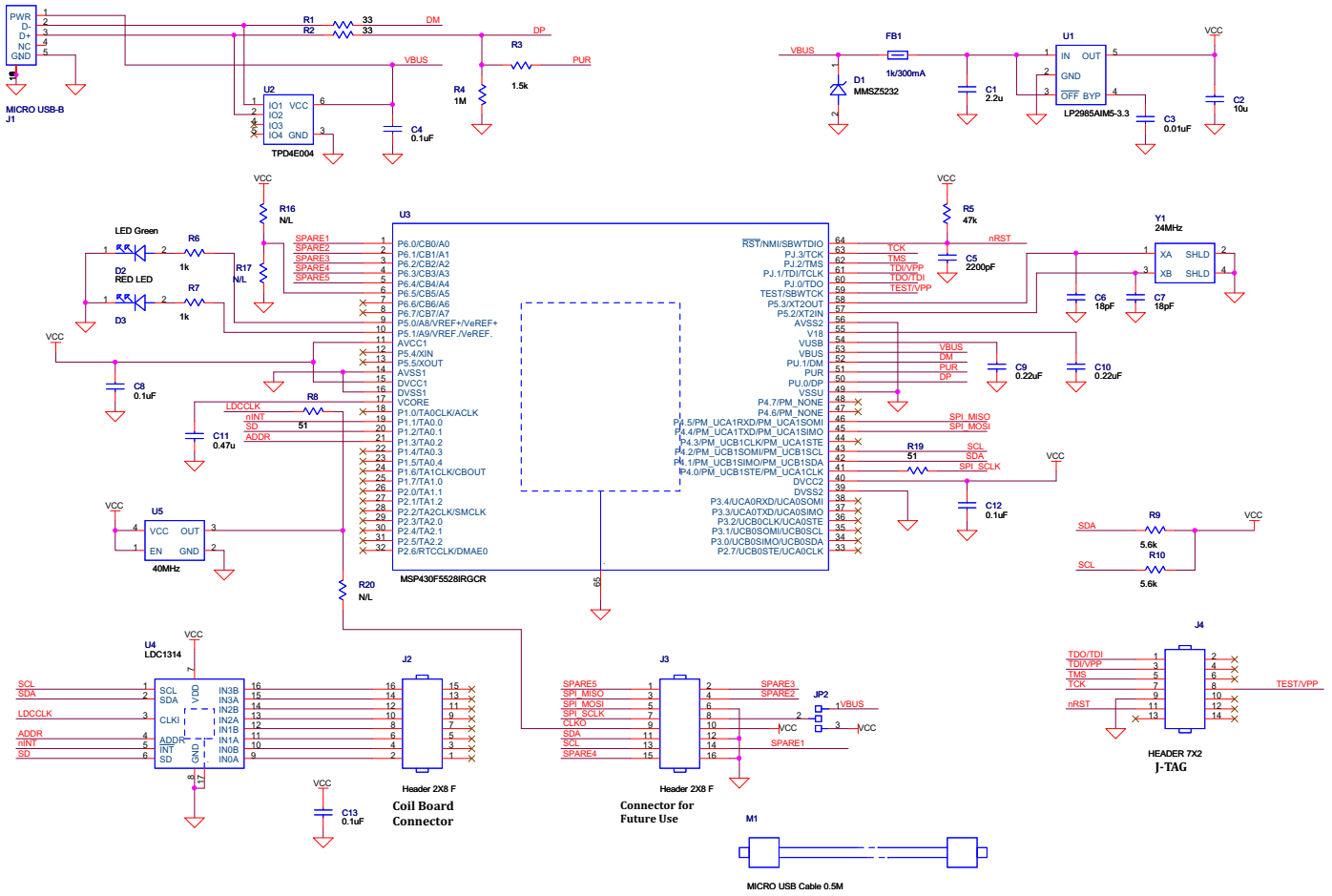

Figure 22. MCU Board Schematic

12.2 Schematics — Coil Board

To download the schematics, see the design files at TIDA-00508.

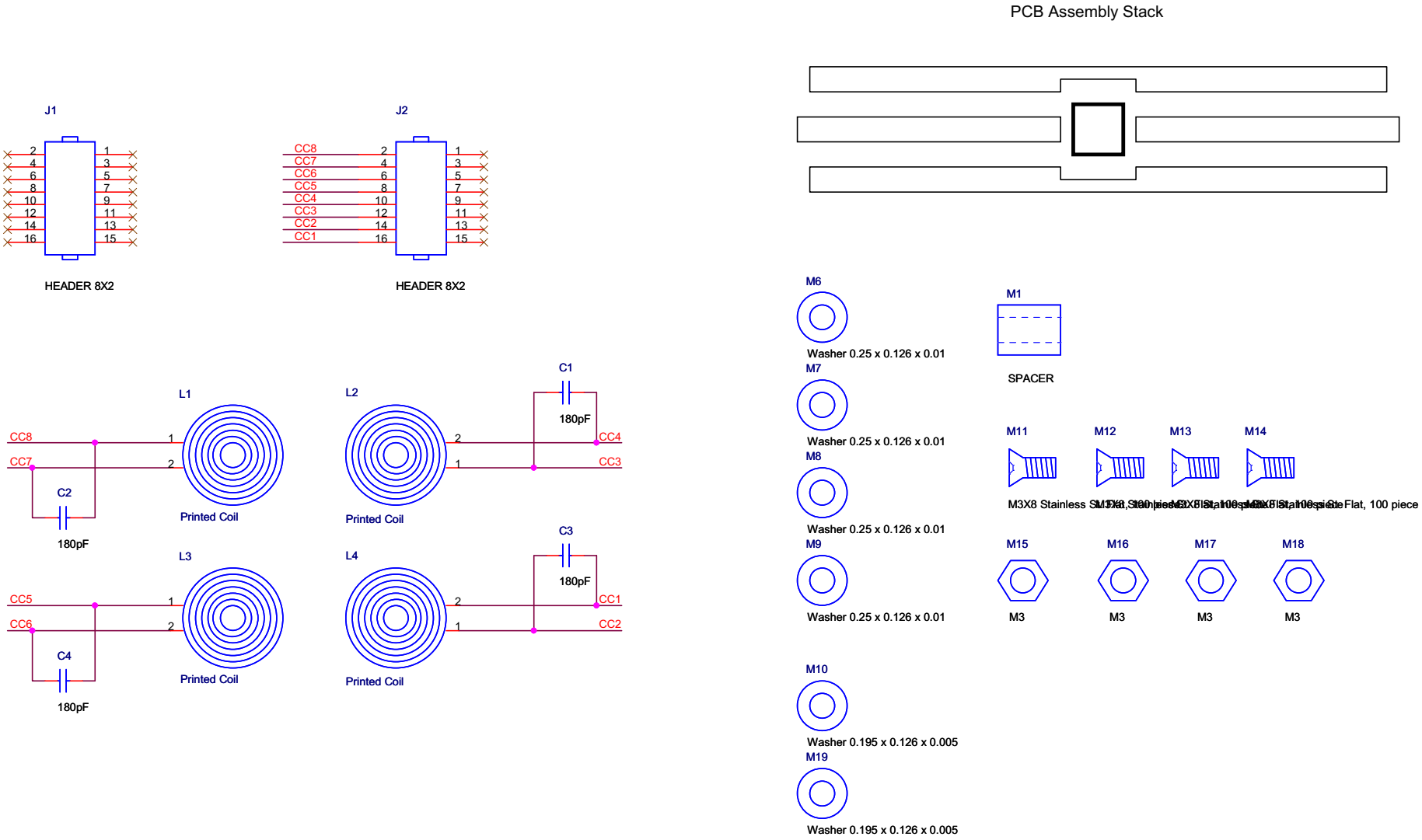

Figure 23. Coil Board Schematic

12.3 Bill of Materials — MCU Board

To download the bill of materials (BOM), see the design files at TIDA-00508.

Table 6. MCU Board BOM

ITEM	QTY	PART REFERENCE	VALUE	DESCRIPTION	MFG1	MFG1_PN
1	1	C1	2.2u	2.2uF 10V X7R 0603 +/-10% -55~125C	muRata	GRM188R71A225KE15D
2	1	C2	10u	CAP,1206,X5R,10uF,+/- 10%, 35V, -55~85C	Taiyo Yuden	GMK316BJ106KL-T
3	1	C3	0.01uF	CAP,0402,X7R,0.01uF,+/- 10%, 25V -55~125C	muRata	GRM155R71E103KA01D
4	4	C4 C8 C12 C13	0.1uF	CAP,0402,X7R,0.1uF,+/- 10%, 16V, -55~125C	Taiyo Yuden	EMK105B7104KV-F
5	1	C5	2200pF	CAP,0402,X7R,2200pF,+/- 10%, 50V	Yageo	CC0402KRX7R9BB222
6	2	C6 C7	18pF	CAP,0402,NPO,18pF,+/- 5%, 50V	TDK	LMK105BJ224KV-F
7	2	C9 C10	0.22uF	CAP,0402,X7R,0.22uF,+/- 10%, 10V, -55~125C	muRata	GRM155R71H222KA01
8	1	C11	0.47u	CAP CER .47UF 25V X7R 0603	muRata	GRM188R71E474KA12D
9	1	D1	MMSZ5232	ZENER 5.6V 500mW	Diodes	MMSZ5232B-7-F
10	1	D2	LED Green	LED Diffused Green High Efficinecy	Osram	LG L29K-G2J1-24-Z
11	1	D3	RED LED	LED 660NM SUPER RED DIFF 0603SMD	Lumex	SML-LX0603SRW-TR
12	1	FB1	1k/300mA	FER 1K @ 100MHz, 0603 300mA 0.6 Ohm	TDK	MMZ1608B102C
13	1	J1	MICRO USB-B	CON, USB, Micro, Type B	FCI	10118193-0001LF
14	2	J2 J3	Header 2X8 F	2MM Header Female SMD BOTTOM ENTRY w. Peg, H=2.8MM	Sullins	NPPN082GFNS-RC
15	1	J4	HEADER 7X2	Heater 7X2,.1X.1, SMD, pin=6.1MM, base-to-pcb=3.56mm	Molex	15912140
16	1	JP2	SOLDER-JUMPER3	Solder Jumper 0201	TBD	TBD
17	2	R1 R2	33	RES,0402,33 OHMS, +/- 5%, 1/16 W	RHOM	MCR01MRTJ330
18	1	R3	1.5k	RES,0402,1.5K OHMS, +/- 5%, 1/16W	Panasonic ECG	ERJ-2GEJ152X
19	1	R4	1M	RES,0402,1M OHMS, +/- 5%, 1/16 W	Panasonic ECG	ERJ-2GEJ105X
20	1	R5	47k	RES,0402,47K OHMS, +/- 5%, 1/16 W	Panasonic ECG	ERJ-2GEJ473X
21	2	R6 R7	1k	RES,0402,1K OHMS, +/- 5%, 1/16 W	Panasonic ECG	ERJ-2GEJ102X
22	2	R8 R19	51	RES,0402,51 OHMS, +/- 5%, 1/16W	Panasonic ECG	ERJ-2GEJ510X
23	2	R9 R10	2.7k	RES,0402,2.7K OHMS, +/- 5%, 1/16W	Stackpole Electronics Inc	RMCF0402JT2K70
24	2	R16 R17	N/L	RES,0402	DO NOT	STUFF
25	1	R20	100	RES,0402,100 OHMS, +/- 5%, 1/16W	Panasonic - ECG	ERJ-2GEJ101X

Table 6. MCU Board BOM (continued)

ITEM	QTY	PART REFERENCE	VALUE	DESCRIPTION	MFG1	MFG1_PN
26	1	U1	LP2985AIM5-3.3	LDO 3.3V 0.15A, VINmax=16V	TI	LP2985AIM5-3.3/NOPB
27	1	U2	TPD4E004	4CH ESD-PROT ARRAY	TI	TPD4E004DRYR
28	1	U3	MSP430F5528IRGCR	MCU 16BIT 128KB FLASH 64VQFN	TI	MSP430F5528IRGCR
29	1	U4	LDC1314	INDUCTANCE TO DIGITAL CONVERTER 4CH	TI	LDC1314
30	1	U5	40MHz	CMOS,40 MHz,SMD 4pin,1.6-3.3V, 50ppm, 5mA	AVX	KC2520B40.0000C10E00
31	1	Y1	24MHz	CRYSTAL 24.000 MHZ 10PF SMD	CTS	403C11A24M00000

12.4 Bill of Materials — Coil Board

To download the bill of materials (BOM), see the design files at TIDA-00508.

Table 7. Coil Board BOM

ITEM	QTY	PART REFERENCE	VALUE	DESCRIPTION	MFG1	MFG1_PN
1	4	C1 C2 C3 C4	180pF	CAP,0402,NPO,180pF,+/- 1%, 50V -55~125C	muRata	GRM1555C1H181FA01D
2	2	J1 J2	HEADER 8X2	8X2 2MM SMD HEADER H=2.2MM Peg=1.2MM	Sullins	NRPN082MAMP-RC
3	4	L1 L2 L3 L4	Printed Coil	8.2MM 2-layer Coil 3.5uH	SVA	TBD
4	1	M1	SPACER	ROUND SPACER ID=0.047" OD=0.125" H=0.125" NYLON	Bivar Inc	939-125
5	5	M6 M7 M8 M9 M10	Washer 0.25 x 0.126 x 0.01	Nylon Washer 0.25 x 0.126 x 0.01	Boker's Inc.	696291
6	4	M11 M12 M13 M14	M3X8 Stainless St. Flat, 100 piece	M3x0.5X8 Stainless St. Flat Head Machine Screw, 100-piece	https://www.boltdepot.com/	Item #6864
7	4	M15 M16 M17 M18	M3	Hex Nuts: M3 X .5MM pitch DIN 934 A2 - 304 Stainless	www.instockfasteners.com	9080032809

12.5 PCB Layout

The correct design of the coil and target is crucial to the success of the rotational sensing using the LDC1314. The design requirement for the coils and the target are described in details in section 6. The following sections describe the PCB layout images of the coil board, target disc board, and the MCU board.

The overall dimensions of the coils and the target can be varied to fit your application as long as the relative dimension requirement is maintained.

To download the layer plots, see the design files at TIDA-00508.

12.5.1 Layout Prints — Target Disc Board

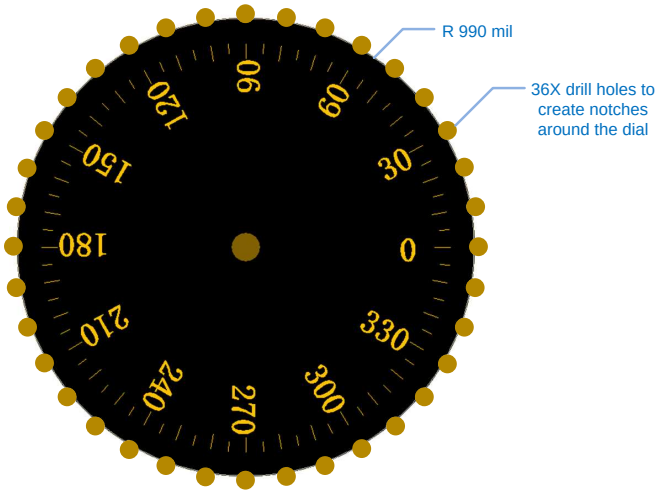

Figure 24. Top Copper and Solder Mask Layers

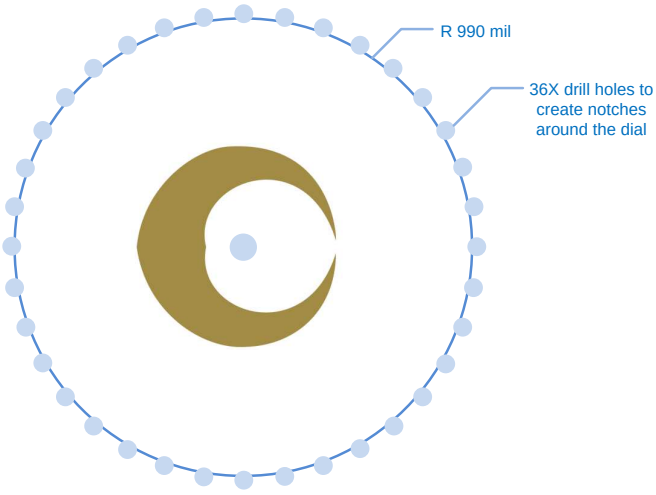

Figure 25. Layer 3 Copper

12.5.2 Layout Prints — Coil Board

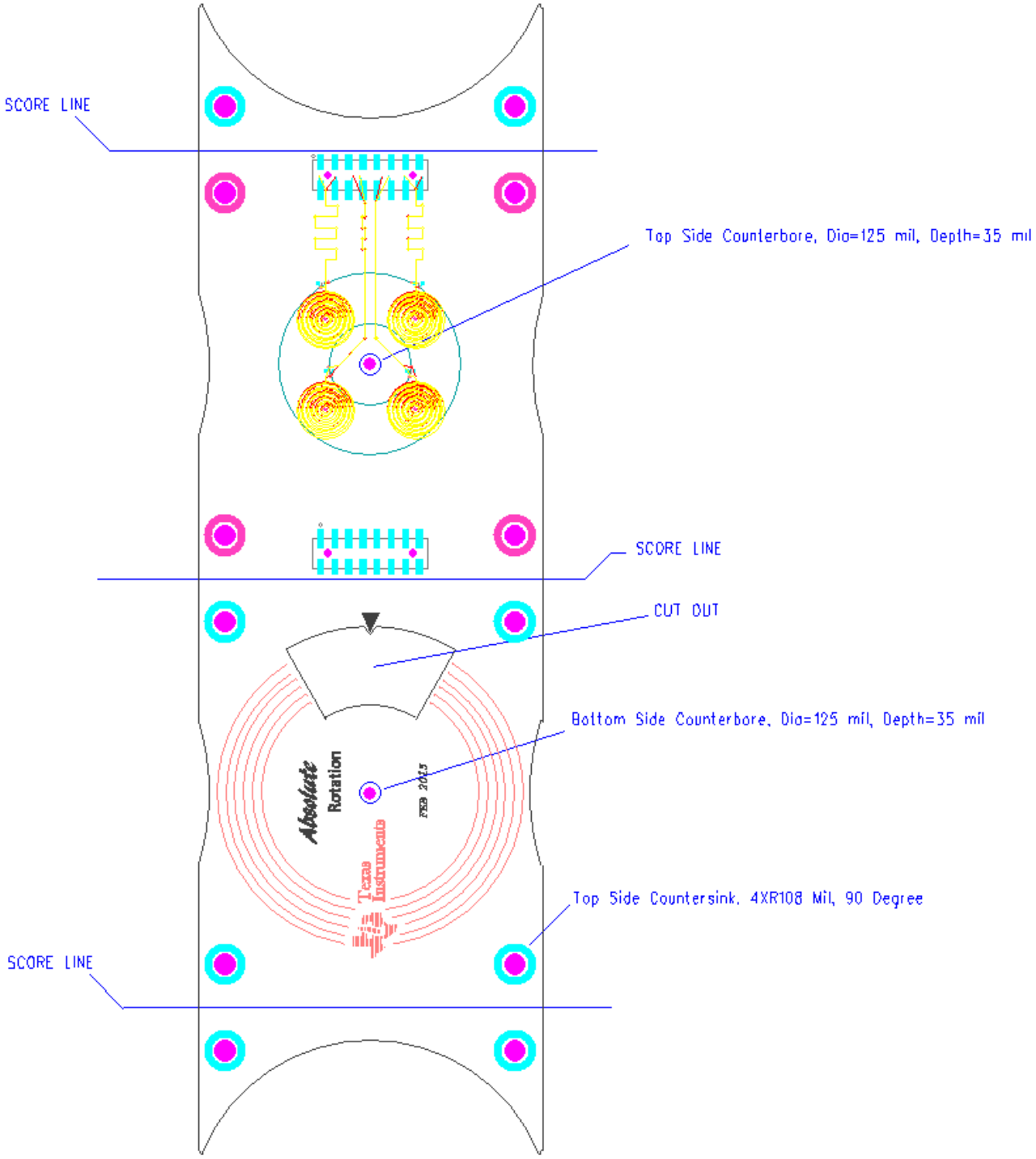

Figure 26. Coil Board Composite View

A differential delay due to unmatched coil trace lengths can cause an oscillation frequency deviation from the LC tank's resonant frequency. The matching of the delays helps minimize the initial frequency errors between the differential sensors. To match the delays, equalize the PCB trace lengths from the LDC1314 to the four sensor coils. This is illustrated in Figure 27.

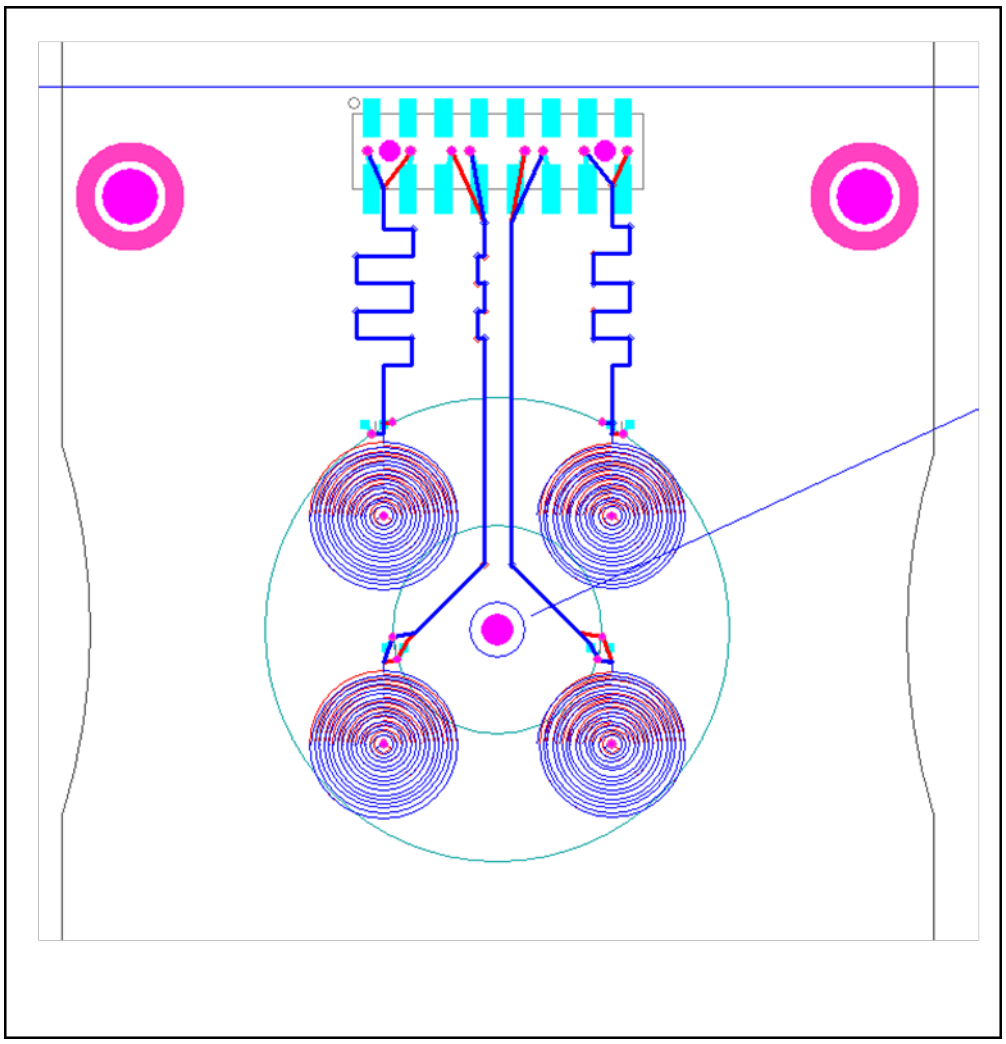

Figure 27. Coil Trace Length Equalization

12.5.3 Layout Prints — MCU Board

Figure 28 shows the composite view of the MCU board layout.

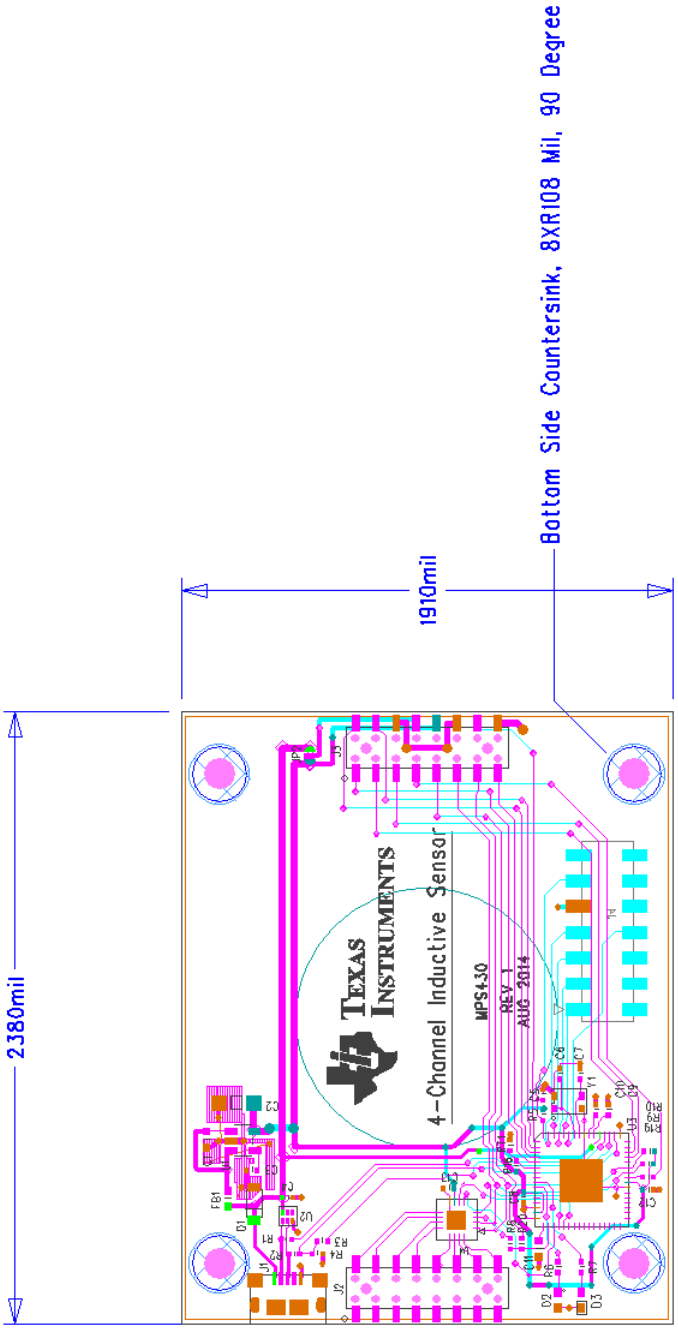

Figure 28. MCU Board Multi-Layer View

12.6 Software Files

To download the software files, see the design files at TIDA-00508.

13 References

1. Texas Instruments, *16-Button Keypad Using the LDC1314 Inductance-to-Digital Converter*, Design Guide (TIDU954).
2. Texas Instruments, *Touch on Metal Buttons With Integrated Haptic Feedback Reference Design*, Design Guide (TIDU613).

14 About the Author

DON LIU a system architect in TI's Precision Signal Path group, located in Santa Clara, California.

Appendix A Measuring R_P of an Inductor

There are several ways to determine the R_P of an inductor, as illustrated in the following figures. Make sure to place the target metal at the closest distance to the coil as required by the application when measuring R_P, for this represents the case of "minimum R_P".

- R_P Measurement Method 1 — Use a network analyzer to measure the complex impedance of the coil (coil only, without the capacitor). The X_L (reactance) and R_S (series loss resistance) values are displayed at a selected frequency. Then use the formula shown in Figure 29 to calculate the R_P.

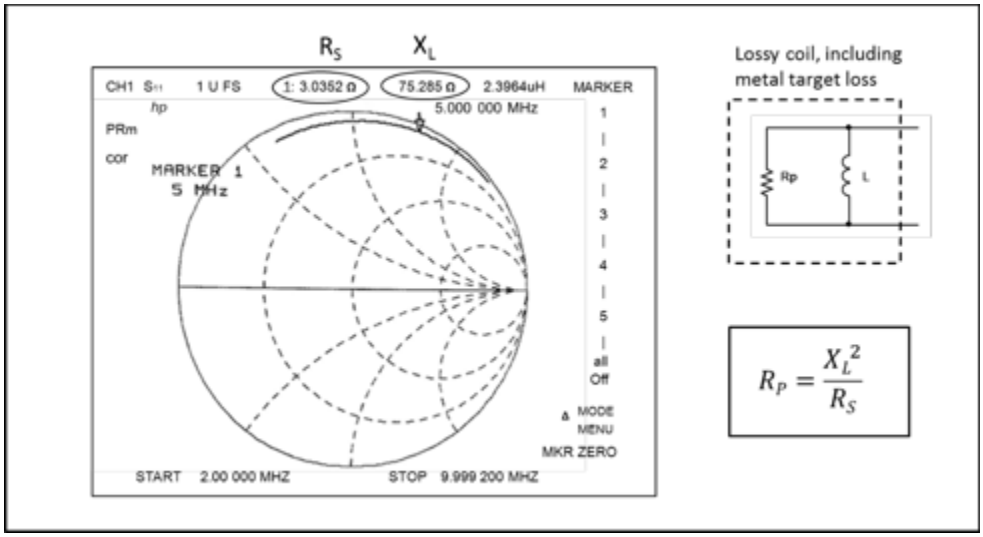

Figure 29. Using a Network Analyzer to Find R_P

- R_P Measurement Method 2 — Use an impedance analyzer to measure the inductance and series resistance of the coil (coil only, without the capacitor). The L_S (Inductance) and R_S (series loss resistance) values are displayed at a selected frequency. Then use the formula shown in Figure 30 to calculate the R_P.

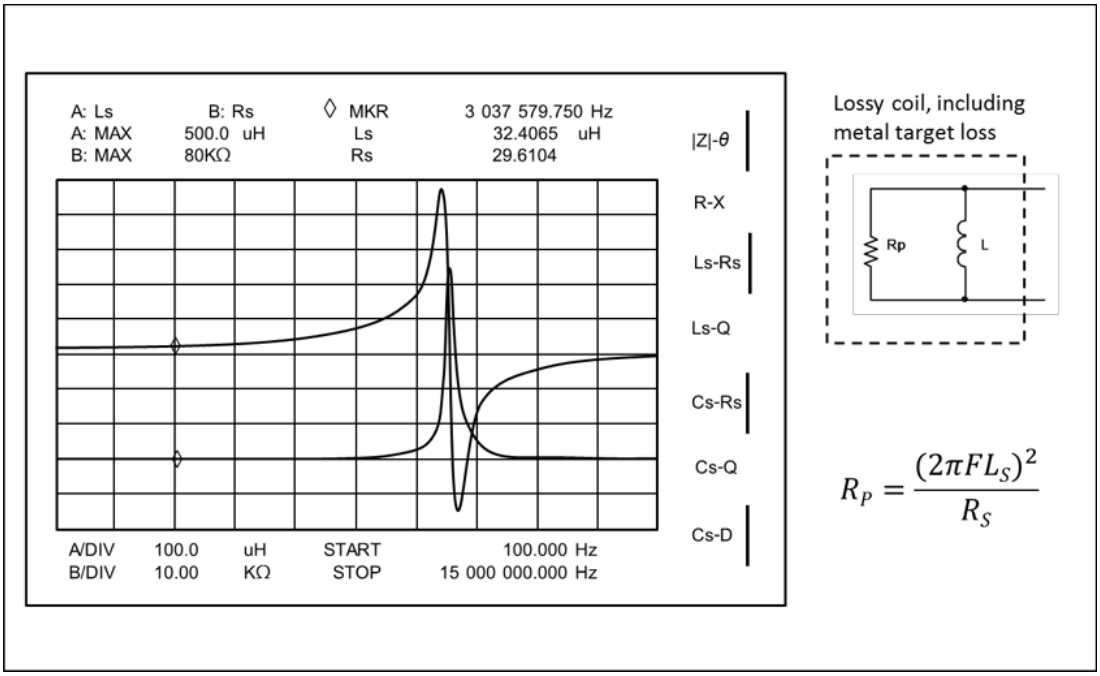

Figure 30. Using an Impedance Analyzer to Find R_P

- R_P Measurement Method 3 — Use a signal generator and oscilloscope as illustrated in Figure 31. The LC tank capacitor is required for this method.

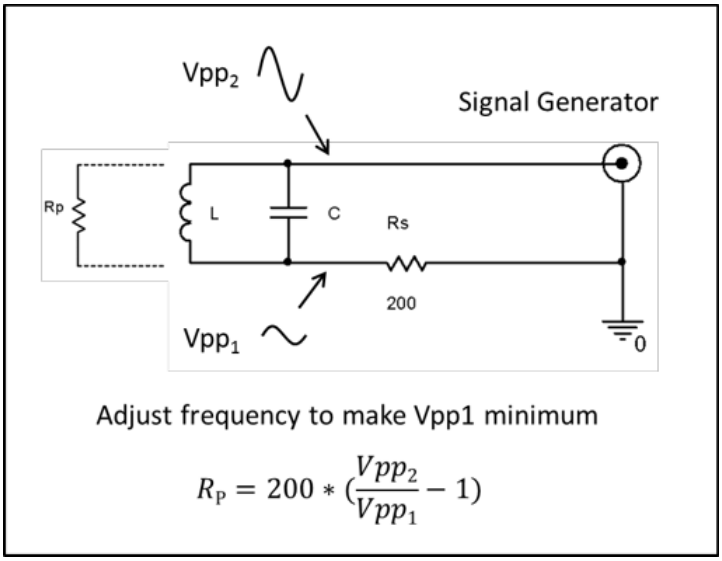

Figure 31. Using a Signal Generator and Oscilloscope to Find R_P

IMPORTANT NOTICE FOR TI DESIGN INFORMATION AND RESOURCES

Texas Instruments Incorporated ('TI") technical, application or other design advice, services or information, including, but not limited to, reference designs and materials relating to evaluation modules, (collectively, "TI Resources") are intended to assist designers who are developing applications that incorporate TI products; by downloading, accessing or using any particular TI Resource in any way, you (individually or, if you are acting on behalf of a company, your company) agree to use it solely for this purpose and subject to the terms of this Notice.

TI's provision of TI Resources does not expand or otherwise alter TI's applicable published warranties or warranty disclaimers for TI products, and no additional obligations or liabilities arise from TI providing such TI Resources. TI reserves the right to make corrections, enhancements, improvements and other changes to its TI Resources.

You understand and agree that you remain responsible for using your independent analysis, evaluation and judgment in designing your applications and that you have full and exclusive responsibility to assure the safety of your applications and compliance of your applications (and of all TI products used in or for your applications) with all applicable regulations, laws and other applicable requirements. You represent that, with respect to your applications, you have all the necessary expertise to create and implement safeguards that (1) anticipate dangerous consequences of failures, (2) monitor failures and their consequences, and (3) lessen the likelihood of failures that might cause harm and take appropriate actions. You agree that prior to using or distributing any applications that include TI products, you will thoroughly test such applications and the functionality of such TI products as used in such applications. TI has not conducted any testing other than that specifically described in the published documentation for a particular TI Resource.

You are authorized to use, copy and modify any individual TI Resource only in connection with the development of applications that include the TI product(s) identified in such TI Resource. NO OTHER LICENSE, EXPRESS OR IMPLIED, BY ESTOPPEL OR OTHERWISE TO ANY OTHER TI INTELLECTUAL PROPERTY RIGHT, AND NO LICENSE TO ANY TECHNOLOGY OR INTELLECTUAL PROPERTY RIGHT OF TI OR ANY THIRD PARTY IS GRANTED HEREIN, including but not limited to any patent right, copyright, mask work right, or other intellectual property right relating to any combination, machine, or process in which TI products or services are used. Information regarding or referencing third-party products or services does not constitute a license to use such products or services, or a warranty or endorsement thereof. Use of TI Resources may require a license from a third party under the patents or other intellectual property of the third party, or a license from TI under the patents or other intellectual property of TI.

TI RESOURCES ARE PROVIDED "AS IS" AND WITH ALL FAULTS. TI DISCLAIMS ALL OTHER WARRANTIES OR REPRESENTATIONS, EXPRESS OR IMPLIED, REGARDING TI RESOURCES OR USE THEREOF, INCLUDING BUT NOT LIMITED TO ACCURACY OR COMPLETENESS, TITLE, ANY EPIDEMIC FAILURE WARRANTY AND ANY IMPLIED WARRANTIES OF MERCHANTABILITY, FITNESS FOR A PARTICULAR PURPOSE, AND NON-INFRINGEMENT OF ANY THIRD PARTY INTELLECTUAL PROPERTY RIGHTS.

TI SHALL NOT BE LIABLE FOR AND SHALL NOT DEFEND OR INDEMNIFY YOU AGAINST ANY CLAIM, INCLUDING BUT NOT LIMITED TO ANY INFRINGEMENT CLAIM THAT RELATES TO OR IS BASED ON ANY COMBINATION OF PRODUCTS EVEN IF DESCRIBED IN TI RESOURCES OR OTHERWISE. IN NO EVENT SHALL TI BE LIABLE FOR ANY ACTUAL, DIRECT, SPECIAL, COLLATERAL, INDIRECT, PUNITIVE, INCIDENTAL, CONSEQUENTIAL OR EXEMPLARY DAMAGES IN CONNECTION WITH OR ARISING OUT OF TI RESOURCES OR USE THEREOF, AND REGARDLESS OF WHETHER TI HAS BEEN ADVISED OF THE POSSIBILITY OF SUCH DAMAGES.

You agree to fully indemnify TI and its representatives against any damages, costs, losses, and/or liabilities arising out of your non-compliance with the terms and provisions of this Notice.

This Notice applies to TI Resources. Additional terms apply to the use and purchase of certain types of materials, TI products and services. These include; without limitation, TI's standard terms for semiconductor products http://www.ti.com/sc/docs/stdterms.htm), evaluation modules, and samples (http://www.ti.com/sc/docs/sampterms.htm).

Mailing Address: Texas Instruments, Post Office Box 655303, Dallas, Texas 75265